Rational Design of Porous Organic Molecules (POMs) Based on B-Heterocyclic Carbenes

Journal:	*Molecular Systems Design & Engineering*
Manuscript ID	ME-ART-11-2020-000156.R1
Article Type:	Paper
Date Submitted by the Author:	14-Dec-2020

Complete List of Authors:	Zhang, Congjie; Shaanxi Normal University, School of Chemistry & Chemical Engineering Tian, Zeqiong; Shaanxi Normal University, School of Chemistry & Chemical Engineering Jia, Wenhong; Shaanxi Normal University, School of Chemistry @ Chemical Engineering Mo, Yirong; Western Michigan University, Chemistry

Design, System, Application Statement

Based on the boron-heterocyclic carbene (BHC) which was proposed by us recently, here we propose and computationally verify a method to design porous organic molecules (POMs), novel 2D covalent organic frameworks (COFs) and metal-organic framework (MOF) using BHC, -C≡C- and Ag-C≡C-Ag as linkers. The uniqueness of the proposed POMs lies in their topologies that are different from those previously reported. The infinite lattices of POMs result in 2D COFs. Further, one of the POMs (POM-25) can be used as polydentate ligands to form 1D layered complexes (C1-C3) with Ag-C≡C-Ag linker to generate MOF. Structures of COFs and MOF have been optimized with the DFT method under the periodic boundary condition. The present computational design provides new ideas for experimentalists in the development of novel COFs and MOFs.

ARTICLE

Rational Design of Porous Organic Molecules (POMs) Based on B-Heterocyclic Carbenes

Received 00th January 20xx,
Accepted 00th January 20xx

DOI: 10.1039/x0xx00000x

Congjie Zhang,*[a] Zeqiong Tian,[a] Wenhong Jia,[a] and Yirong Mo*[b]

We have rationally designed and computationally verified 36 porous organic molecules (POMs), 3 types of novel 2D covalent organic frameworks (COFs) and one kind of metal-organic framework (MOF) based on the B-heterocyclic carbene (BHC) building blocks associated with -C≡C- and Ag–C≡C–Ag linkers. The topologies of POMs are notably different from those previously reported. More interestingly, the hexagon channels of POMs are almost regular hexagons though the edges of the hexagon channels are not exactly the same. Among POMs, those with apertures of 7.2, 11.5 and 16.1 Å are predicted to be stable. The infinite lattices of POMs result in 3 types of 2D COFs (COF-BHC-n, n=1-3), whose symmetry is approximately hexagonal. The first electron spectra of the 36 POMs calculated with the TD-B3LYP/6-31G** method range from 325.0 to 482.0 nm and strongly depend on the structures and sizes. Thus, the proposed POMs might be potential optical materials due to the wide range of spectra. Further, one of the POMs (POM-25) can be used as polydentate ligands to form 1D layered complexes (C1-C3) with Ag–C≡C–Ag linkers. The infinite lattices of C1-C3 result in a kind of 1D MOF (MOF-BHC-1). Analyzing the lengths in C1-C3 and MOF-BHC-1, as well as the Wiberg bond indices (WBIs) in C1-C3, we found that MOF-BHC-1 contains plenty of planar tetracoordinate carbons (ptCs). Thus, we have introduced ptCs into the field of MOF and developed a method of obtaining MOFs with new topologies from POMs.

Introduction

Porous organic molecular materials have attracted intensive attentions owing to their unique chemical properties and broad applications in storage, catalysis, molecular separations and so on.[1-5] Their structures can be classified with intrinsic and extrinsic porosities from the standpoint of applications.[5] Intrinsically porous organic molecules (POMs) have open, bowl- or ring-shaped cavities, such as calix[n]arenes,[1] cucurbit[n]urils[2] and pillar[n]arenes[4]. When organic molecules pack into solids inefficiently to create voids or channels, such solids are distinguished with the extrinsic porosity as pores are located between molecules. More recently, however, covalent organic frameworks (COFs) have been considered to be a novel class of intrinsically porous and crystalline materials composed of entirely light elements (H, B, C, N, and O) through strong covalent bonding.[6,7] These materials are characterized with periodic network structures extended in two or three dimensions (2D or 3D), which were atomically obtained by building blocks. Since first reported by Yaghi and co-workers in 2005,[8] COFs have drawn enormous interests in both experimental and theoretical domains owing to their outstanding thermal stability, high surface area and low density, as well as their potential applications in energy storage,[9,10] catalysis[10,11] and optoelectronic devices.[12] Based on the shapes of the hole channels, POMs can be classified into hexagon, square, rhombus, triangular shapes, and so on.[7] But if the topology patterns are the focus for designing 2D COFs,[7] there are generally four kinds of protocols for constructing POMs with the hexagon shape as shown in Scheme 1.

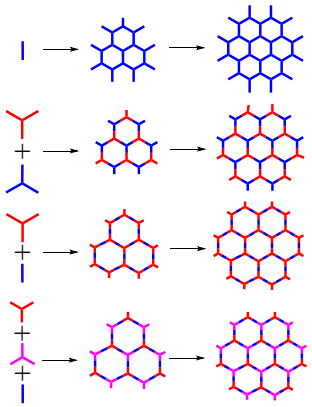

Scheme 1. Four different protocols for constructing porous organic molecules (POMs) with hexagonal channels.

Apart from COFs, there is another class of much popular porous crystalline materials, namely metal-organic frameworks (MOFs).[13,14] MOFs are one-, two- or three-dimensional structures with infinite lattices composed of metal cations or clusters that serve as multitopic inorganic nodes with polydentate organic ligands acting as linkers. The pioneering

[a] Key Laboratory of Macromolecular Science of Shaanxi Province, School of Chemistry & Chemical Engineering, Shaanxi Normal University, Xi'an, 710062, China.
[b] Department of Nanoscience, Joint School of Nanoscience and Nanoengineering, University of North Carolina at Greensboro, Greensboro, NC 27401, United States.
† Footnotes relating to the title and/or authors should appear here.
Electronic Supplementary Information (ESI) available: [details of any supplementary information available should be included here]. See DOI: 10.1039/x0xx00000x

works of MOF constructions and applications can be traced back to the reports by the Yaghi group in the 1990s.[15] Up to now, more than 20,000 MOF structures have been synthesized and extensively applied in fields such as hydrogen storage, textile industries, transportation, all-electric automobile prototypes, food packaging, and respiratory systems.[14,16]

Examining and comparing the general structures of POMs, COFs and MOFs, we wonder whether there is any alternative protocol for designing novel POMs with hexagons in addition to the current four kinds shown in Scheme 1. Further, is there any possibility to construct MOFs by linking POMs through metal cations?

Recently, we proposed a family of interesting molecules, i.e. the derivatives of 2-borabicyclo[1.1.0]but-1(3)-ene (2BB). While these molecules remain elusive experimentally, their structures, bonding nature and reactivity have been theoretically investigated and validated.[17, 18] Study with the ab initio valence bond (VB) method showed that the substituted 2BBs have carbene characters. As such, they are termed as B-heterocyclic carbenes (BHCs, shown in Scheme 2).[19] Notably, BHCs can act as ligands to form complexes with transition metals. These metal complexes not only contain a planar tetracoordinate carbon (ptC),[17] but also can be promising catalysts.[18] We note that there is another link between molecules with ptC atoms and carbenes as reported by Thimmakondu's group.[20] They theoretically obtained the isomerization of high-energy structures of C_7H_2 with a ptC atom to an experimentally known ring-chain carbene, 1-(buta-1,3-diynyl)-cyclopropenylidene. In present work, we intended to design building blocks formed by two and three BHC units, and link these building blocks together with -C≡C- and Ag–C≡C–Ag linkers. In this way, we demonstrated a protocol for designing novel POMs with hexagons and an interesting example of constructing MOF with POMs, as well as 2D COFs.

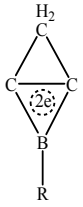

Scheme 2. Substituted 2-borabicyclo[1.1.0]but-1(3)-ene or B-heterocyclic carbene (BHC).

Computational Methods

All density functional theory (DFT) computations were performed with the B3LYP functional in combination with the SDD basis sets[21] for silver and 6-31G** basis sets[22] for H, B and C atoms. Optimized structures were verified with zero imaginary vibrational frequencies. In order to evaluate the reliability of this B3LYP functional[23] together with 6-31G** basis set, we also performed computations for the building blocks and small POMs using the M06-2X functional[24] together with the 6-311+G** basis set.[25] Both the B3LYP/6-31G** and M06-2X/6-311+G** theoretical levels generate comparable optimal geometries for small systems. Wiberg bond indices (WBIs) for the POMs and complexes were derived from the natural bond orbital (NBO) analysis.[26] The vertical electronic absorption spectra of the POMs were obtained by means of the time-dependent density functional theory at the TD-B3LYP/6-31G** level. The COFs and MOF were optimized with the relativistic local spin density approximation (RLSDA) method under the periodic boundary condition (PBC). All calculations in this work were performed with the Gaussian09 program.[27]

Results and Discussion

Experimentally, four kinds of topologies of POMs with hexagonal channels have been reported so far as shown in Scheme 1. Here we propose additional kinds of POMs based on the BHC building blocks and -C≡C- linkers which are illustrated in Schemes 3. The red and blue building blocks in Scheme 3 represent BHCs building blocks and -C≡C- linkers, respectively. In order to better describe the topologies of POMs shown in Schemes 1 and 3, we used the ratio of the numbers of different building blocks as an index. Of particular, our focus is on the structures whose three hexagonal channels arrange like phenalene because such structures are sufficient to distinguish the topologies of the POMs. For instance, the ratios of the numbers of the building blocks used to construct the four POMs in Scheme 1 are 1 (only one type of building block), 6:7 and 13:15 (two types of building blocks), as well as 6:7:15 (three types of building blocks), respectively. Similarly, the ratios of the numbers of the building blocks for the examples of two new POMs **F** and **L** in Scheme 3 are 4:6 and 1:3:6, respectively. We note that the ratios for **F** and **L** are smaller than for the POMs in Scheme 1. In fact, the POMs in Scheme 3 have simpler topology than those in Scheme 1. As seen from Scheme 3, the combinations of building blocks leads to two different kinds of POMs. One kind of POMs (**a**) have BHC units on the outside of hexagons, while the other (**b**) does not contain BHC units on the outside of hexagons. In addition, there are two types of edges of the hexagons in POMs. One type of edges (red and magenta edges) have BHC units, while the other (blue edges) does not contain BHC units. Fortunately, the lengths of these two types of different edges in the hexagonal channels are very close, indicating that the hexagonal channels of the POMs in Scheme 3 are approximatively regular hexagon.

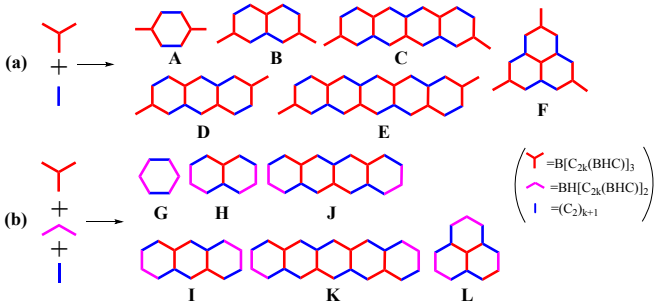

Scheme 3. Porous organic molecules (POMs) with hexagonal channels constructed by BHCs.

We considered six building blocks constructed by two or three BHCs, namely $BH[(C_2)_k(BHC)]_2$ and $B[(C_2)_k(BHC)]_3$ (k=0-2). Because the molecular skeleton of BHC is planar, each of $BH[(C_2)_k(BHC)]_2$ or $B[(C_2)_k(BHC)]_3$ has two isomers. In one isomer, the rhombuses of the BHC units are coplanar, while in the other the rhombuses of the BHC units are perpendicular to the plane formed by the four boron atoms. B_n-c and B_n-p (n=1-6) represent the co-planar and perpendicular structures of $B[(C_2)_k(BHC)]_3$ and $BH[(C_2)_k(BHC)]_2$, respectively. Using the M06-2X/6-311+G** and B3LYP/6-31G** methods, all 12 structures of $B[(C_2)_k(BHC)]_3$ and $BH[(C_2)_k(BHC)]_2$ (k=0-2) have been optimized and illustrated in Fig. 1. The relative energies of two isomers of either $B[(C_2)_k(BHC)]_3$ or $BH[(C_2)_k(BHC)]_2$ are listed in Table 1S (see Supporting Information) and Fig.1. Computations show that B_n-p is more stable than B_n-c by 9.8, 3.4, 1.6, 6.2, 2.5 and 1.1 kcal·mol^{-1}, respectively, at the M06-2X/6-311+G** level. Similar results can be obtained at the B3LYP/6-31G** level. Thus, the steric effect is more pronounced than the conjugation effect in determining the preferred conformations of $BH[(C_2)_k(BHC)]_2$ and $B[(C_2)_k(BHC)]_3$. Moreover, the relative energies decrease with the increasing k value, indicating that the steric effect diminishes with the BHC units moving away. Calculated vibrational frequencies of $BH[(C_2)_k(BHC)]_2$ and $B[(C_2)_k(BHC)]_3$ show that B_n-p structures have no imaginary frequency, while B_n-c structures have two or three imaginary frequencies. Thus, B_n-p are situated at the minima on the potential energy surfaces and electronically stable. Results from the M06-2X and B3LYP computations are essentially the same, and the optimized lengths between $C(H_2)$ and the center boron atom of B_n-p (n=1-6) are 4.21, 6.76, 9.33, 4.21, 6.76 and 9.34 Å, respectively. On the basis of optimized geometries and relative energies of $BH[(C_2)_k(BHC)]_2$ and $B[(C_2)_k(BHC)]_3$ obtained at the B3LYP/6-31G** and M06-2X/6-311+G** levels, we conclude that the B3LYP approach is reliable for the calculations of BHC systems.

According to the topology of the POMs in Scheme 3(**a**), the red building blocks $B[(C_2)_k(BHC)]_3$ (k=0-2, corresponding to B_n-p with n=1-3) and blue building blocks $(C{\equiv}C)_{k+1}$ are assembled to six types of POMs **A**-**F**. The topology of these POMs is that two B_n-p building blocks with the two-two opposite mode form a hexagonal channels via two C≡C linkers. Consequently, with three different k values (0-2), there are totally 18 different POMs can be constructed following the assembly mode in Scheme 3(**a**), which is denoted as POM-n (n=1-18). Optimized geometries of POM-n (n=1-18) are shown in Fig. 2. For POM-n (n=1-6) where k=0, the apertures of the hexagonal channels are in the range of 7.2-7.4 Å, with the largest one in POM-6. The apertures of the hexagonal channels situated at the two sides of POM-n (n=3-5) are slightly smaller than those of middle hexagonal channels, which give rise from the edges on the outside of the hexagons. The lengths of edges of the hexagonal channels in different POM-n systems are slightly varied, and are close to 4.22 and 4.11 Å, respectively. Thus, the hexagonal channels in POM-n (n=1-6) can be approximated as regular hexagons. To verify the B3LYP/6-31G** results, POM-n (n=1-2) were also optimized at the M06-2X/6-311+G** level. Both levels lead to comparable optimal geometries. Since geometry optimizations of BHC-based POMs by the M06-2X method must use high precision integral lattice points to avoid small imaginary frequencies, for the sake of computational costs, we used the B3LYP/6-31G** method for all following computations.

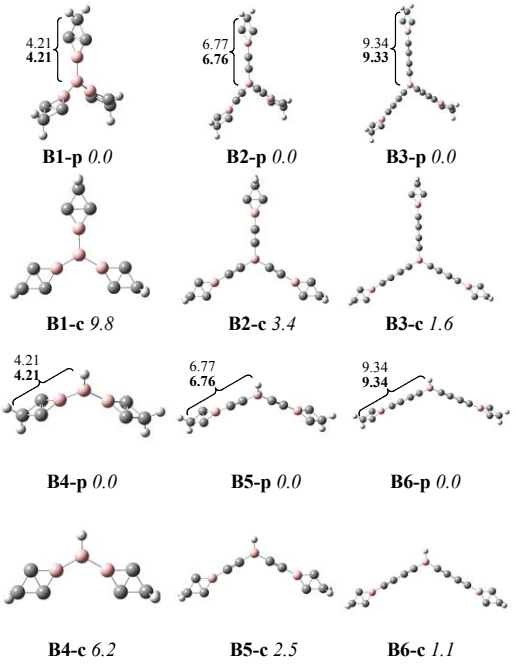

Figure 1. Comparison of the optimized lengths (in angstrom) between C(H2) and the central B atom in BHC components of the perpendicular structures of B[(C2)k(BHC)]3 and BH[(C2)k(BHC)]2 at the B3LYP (in plain) and M06-2X (in bold) levels, as well as the relative energy (in italic, in kcal·mol^{-1}) at the M06-2X level.

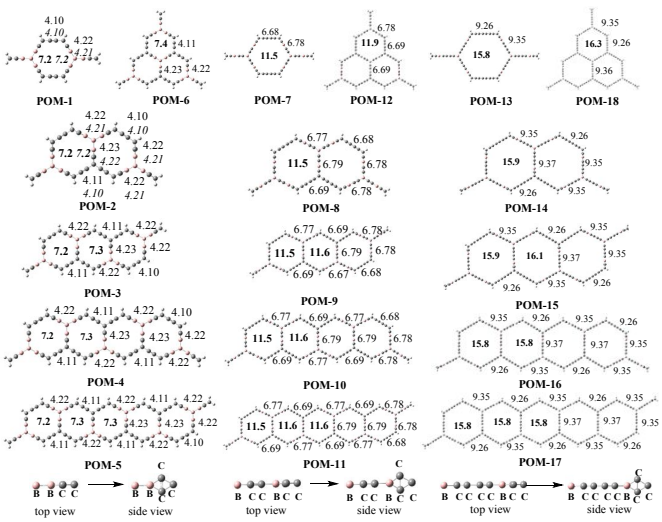

Figure 2. Optimized side lengths (in plain, angstrom) and apertures (in bold, angstrom) of the hexagonal channels of POM-n (n=1-18) at the B3LYP level, compared with the data in italic at the M06-2X level. The side views of the edges are given in the bottom of the figure.

For POM-n (n=7-12 and n=13-18), due to the addition of -C≡C- linkers, the apertures are much larger than those of n=1-6 by about 4.3 and 8.9 Å, and close to 11.7 to 16.2 Å, respectively. The lengths of the two types of edges of the hexagonal channels POM-n (n=7-12 and n=13-18) are around 6.68 and 6.78 Å, as

well as 9.25 and 9.36 Å respectively. The small difference (0.10 for n=7-12 or 0.11 Å for n=13-18) between these two types of edges once again suggests that the hexagonal channels are approximately regular hexagons. The lengths of the edges containing BHC units of the hexagonal channels are close to those in B_2-p and B_3-p, indicating that the assembly of B_2-p and B_3-p have little influence on their structures.

As can be seen from Scheme 3(**a**) and Fig. 2, the first five POMs of each set (n=1-5, 7-11, 13-17) are structurally similar with the derivatives of acene, while POM-6, POM-12 and POM-18 are structurally similar with the derivatives of phenalene. When the edges on the outside of the hexagons of **A**-**F** in Scheme 3(**a**) were replaced with hydrogen atoms, another kind of POMs was obtained and illustrated in Scheme 3(**b**). The POMs **G**-**L** are constructed by three building blocks and structurally similar with acene and phenalene. Following the protocol in Scheme 3(**b**), we can similarly construct 18 POMs by assembling B_n-p (n=1-6; 1-3 in red for $B[(C_2)_k(BHC)]_3$ and 4-6 in magenta for $BH[(C_2)_k(BHC)]_2$ in Scheme 3) and $(C{\equiv}C)_{k+1}$ (in blue in Scheme 3) building blocks which are labeled with POM-n (n=19-36). Optimized structures of these POM-n (n=19-36) are illustrated in Fig. 3. Among these 18 POMs, the first 6 members POM-n (n=19-24) are assembled by B_1-p, B_4-p and -C≡C- blocks, and have the lengths of edges and apertures very close to those of POM-n (n=1-6) in Fig. 2. Thus, the replacements of B_1-p with B_4-p have little influence on the structures of POMs. Similar results can be found between POM-n (n=7-18) in Fig. 2 and POM-n (n=25-36) in Fig. 3. The lengths of edges and apertures of the latter (n=25-30 and n=31-36) are about 6.73 and 11.6, as well as 9.31 and 16.1Å, respectively.

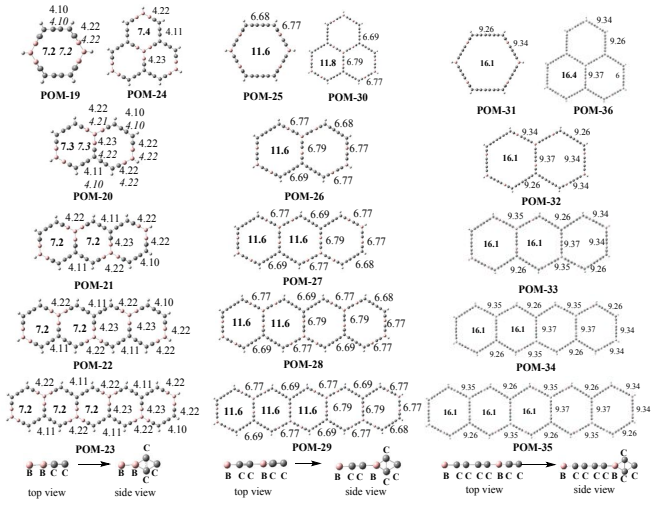

Figure 3. Optimized side lengths (in plain, angstrom) and apertures (in bold, angstrom) of the hexagonal channels of POM-n (n=19-36) at the B3LYP level, compared with the data in italic at the M06-2X level. The side views of the edges are given in the bottom of the figure.

Considering that POM-n (n=1-36) are structurally polycyclic, we calculated their first vertical electron energies by the TD-B3LYP/6-31G** method in order to investigate the electronic properties with the increasing size of POMs. Results including vertical transition energies, transition states and oscillator strengths were listed in Table 2S (in Supporting Information). Fig. 4 also illustrates the changes of the vertical transition energies of POM-n with respect to n. Clearly, the transition energies strongly depend on the structures and sizes, and decrease with the increasing of the aperture of POM-n. For example, the transition energies of POM-n (n=19, 25 and 31) are 319.31, 349.67 and 413.47 nm, respectively, whereas similar structures exhibit very close transition energies. Indeed, the differences of the transition energies among POM-n (n=1-6) and POM-n (n=19-24) are less than 6.00 nm. The transition energies of the POM-n which are structurally similar with acene have a zig-zag alternation feature with the increase of the size. For example, the transition energies of the POM-n (n=1-5) are 325.03, 341.73, 338.45, 348.69 and 346.53 nm, respectively. Because POM-n have wide spectra of ranging from 319.0 to 488.0 nm, the POMs might be potential optical materials.

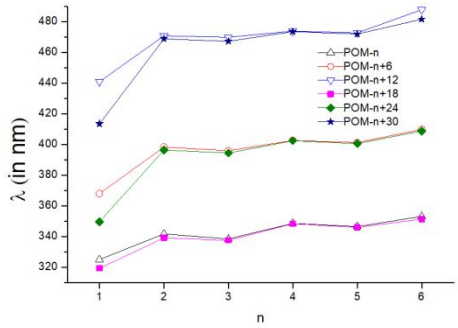

Figure 4. First vertical transition energies (λ, in nm) of POM-n with respect to n.

According to the correlation between the apertures and structures of POM-n (n=1-36), each additional -C≡C- unit in the B_n-p building blocks results in the increasing of the aperture of the subsequent BHC-based POMs by about 4.4 Å. Consequently, the apertures of POM-6, POM-12 and POM-18 are 7.4, 11.9 and 16.3 Å, respectively. In fact, we can design BHC-based POMs with even larger apertures as long as the B_n-p building blocks are extended by adding more -C≡C- units. More interestingly, when POM-n (1-18) are extended to 2D structures with infinite lattices, three types of COFs can be constructed. Optimized apertures and lattice parameters of COF-BHC-n (n=1-3) at the RLSDA/6-31G** level with PBC were illustrated in Fig. 5. As seen from Fig. 5, the apertures of COF-BHC-n (n=1-3) are around 7.2, 11.5 and 15.9, respectively, consistent with that of the corresponding POMs. The angles of the lattice parameters of COF-BHC-n (n=1-3) are close to 60.0°, in addition, the lengths of the edges of the lattice are the same. Thus, the 2D COF-BHC-n (n=1-3) are of hexagonal lattices. As shown in Scheme 3(**a**), the topological structures of such COFs are different from those in literature,[15] suggesting a kind of COF with novel topology.

Because the carbene units in POM-n (n=1-36) can be polydentate ligands to form 1D layered complexes, we can assemble POM-n with transition metal linkers to obtained MOFs. Herein, we first designed three complexes (**C1**-**C3**) by putting POM-25 molecules together with Ag–C≡C–Ag linkers to verify the rationality of such assembling. Optimized structures of **C1**-**C3** at the B3LYP level were illustrated in Fig. 6. Computations showed that **C1**-**C3** have no imaginary frequencies. Their apertures and edge lengths of hexagonal

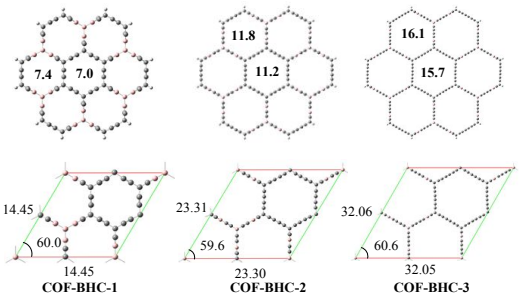

Figure 5. Optimized apertures (in bold, angstrom) and lattice parameters (in plain) at the RLSDA/6-31G** level with the periodic boundary condition (PBC).

channels are 11.6 and 6.67-7.79 Å, respectively, which are well consistent with those of POM-25. Thus, there is little structural variation for POM-25 molecules when they are assembled by the transition metal silver to form complexes. The lengths and WBIs of the selected bonds in **C1**-**C3** were listed in Tables 3S which shows that the lengths of ptC-Ag, ptC-B, ptC-C(CH) and ptC-C in **C1**-**C3** are 2.11, 1.52, 1.54 and 1.47 Å, respectively. Besides, the WBIs of the ptC-Ag, ptC-B, ptC-C(CH) and ptC-C bonds in **C1**-**C3** are 0.31, 0.94, 0.87 and 1.26, respectively. Thus, Ag^+ and POM-25 can form effective coordination bonds in **C1**-**C3**. Notably, the carbon atoms in **C1**-**C3** bonded to Ag^+ are ptCs. When adding POM-25 to the complex **C3** infinitely, a kind of one-dimension MOF (MOF-BHC-1) can be obtained. Optimized structure of MOF-BHC-1 using the RLSDA method under PBC was also plotted in Fig. 6. Calculated apertures, edge lengths of hexagonal channels and the layer spacing in MOF-BHC-1 are well consistent with those in **C1**-**C3**, indicating the infinite lattice formed by POM-25 with Ag–C≡C–Ag linkers is feasible. The lengths of ptC-Ag, ptC-B, ptC-C(CH) and ptC-C bonds in MOF-BHC-1 are very close to those of **C1**-**C3**, showing that MOF-BHC-1 contains plenty of ptCs. Since the compounds with ptCs were envisioned first by Hoffman,[28] ptCs have been identified in small organic molecules, clusters, nanotubes and complexes.[29] Here we have rationally designed MOF-BHC-1 which contains plenty of ptCs. In other words, ptCs have been introduced into popular MOF. Furthermore, we have established a relationship between POMs and MOF on the basis of BHCs building blocks. The BHC-based POMs, COFs and MOF are promising functional materials due to their unique topologies.

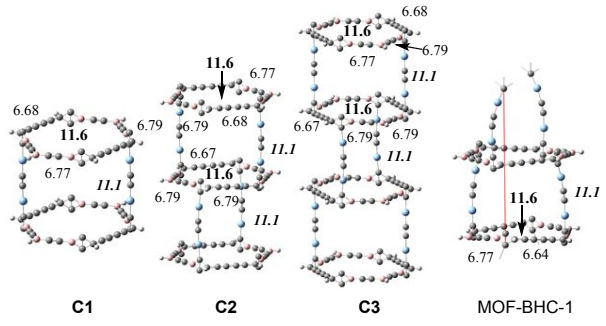

Figure 6. Optimized side lengths (in plain), layer spacing (in bold and italic) and the apertures (in bold) of the hexagonal channels of **C1**-**C3** and MOF-BHC-1. All data are in angstroms.

Conclusions

Using six types of B-heterocyclic carbenes (BHC), namely $B[(C_2)_k(BHC)]_3$ and $BH[(C_2)_k(BHC)]_2$ (k=0-2), and -C≡C- building blocks in addition to Ag–C≡C–Ag linkers, we have theoretically proposed and analyzed thirty-six novel POMs, three COFs and one MOF. Calculated results showed that the topologies of these POMs, COFs and MOF are significantly different from those that have been reported experimentally so far. The edges of the hexagonal channels in POMs and COFs are variable and depend on the number of -C≡C- linkers, but the hexagons themselves are nearly regular hexagons. The POMs and COFs that are structurally similar with polynuclear aromatic compounds have been predicted to be stable. The first electron transition energies of the POM-n decrease with the increase of the apertures. The transition energies of 1D POM-n have a zig-zag alternation feature. The spectra of POM-n (n=1-36) are in the range of 325.0-482.0 nm, suggesting that the proposed POM-n might be potential optical materials due to the wide range of spectra. The POM-25 can be polydentate ligands to form stable MOF with the linkers of Ag–C≡C–Ag. The carbon atoms of the BHC units in MOF-BHC-1 bonding to Ag^+ are ptCs. In brief, we theoretically designed novel stable BHC-based POMs, COFs and MOF, introduced ptCs into the field of MOF, as well as established a correlation among POMs, COFs and MOFs.

Conflicts of interest

There are no conflicts to declare.

Acknowledgements

The authors thank the National Natural Science Foundation of China for financial support (No. 21373133). This work was performed in part at the Joint School of Nanoscience and Nanoengineering, a member of the Southeastern Nanotechnology Infrastructure Corridor (SENIC) and National Nanotechnology Coordinated Infrastructure (NNCI), which is supported by the National Science Foundation (Grant ECCS-1542174).

Notes and references

1 J. L. Atwood, L. J. Barbour and A. Jerga, *Science*, 2002, **296**, 2367-2369; J. L. Atwood, L. J. Barbour, A. Jerga and B. L. Schottel, *Science*, 2002, **298**, 1000-1002.
2 S. Lim, H. Kim, N. Selvapalam, K. J. Kim, S. J. Cho, G. Seo and K. Kim, *Angew. Chem. Int. Ed.*, 2008, **47**, 3352-3355.
3 S. Das, P. Heasman, T. Ben and S. L. Qiu, *Chem. Rev.*, 2017, **117**, 1515-1563.
4 K. C. Jie, M. Liu, Y. J. Zhou, M. A. Little, A. Pulido, S. Y. Chong, A. Stephenson, A. R. Hughes, F. Sakakibara, T. Ogoshi, F. Blanc, G. M. Day, F. H. Huang and A. I. Cooper, *J. Am. Chem. Soc.*, 2018, **140**, 6921-6930; E. R. Li, K. C. Jie, Y. J. Zhou, R. Zhao and F. H. Huang, *J. Am. Chem. Soc.*, 2018, **140**, 15070-15079.
5 M. A. Little and A. I. Cooper, *Adv. Funct. Mater.*, 2020.
6 A. P. Cote, H. M. El-Kaderi, H. Furukawa, J. R. Hunt and O. M. Yaghi, *J. Am. Chem. Soc.*, 2007, **129**, 12914-12915; H. M. El-Kaderi, J. R. Hunt, J. L. Mendoza-Cortes, A. P. Cote, R. E. Taylor,

M. O'Keeffe and O. M. Yaghi, *Science*, 2007, **316**, 268-272; J. R. Hunt, C. J. Doonan, J. D. LeVangie, A. P. Cote and O. M. Yaghi, *J. Am. Chem. Soc.*, 2008, **130**, 11872-11873; P. Kuhn, M. Antonietti and A. Thomas, *Angew. Chem. Int. Ed.*, 2008, **47**, 3450-3453; S. Wan, J. Guo, J. Kim, H. Ihee and D. L. Jiang, *Angew. Chem. Int. Ed.*, 2009, **48**, 5439-5442; S. Y. Ding and W. Wang, *Chem. Soc. Rev.*, 2013, **42**, 548-568; H. Xu, J. Gao and D. L. Jiang, *Nat. Chem.*, 2015, **7**, 905-912; J. L. Segura, M. J. Mancheno and F. Zamora, *Chem. Soc. Rev.*, 2016, **45**, 5635-5671; E. Q. Jin, M. Asada, Q. Xu, S. Dalapati, M. A. Addicoat, M. A. Brady, H. Xu, T. Nakamura, T. Heine, Q. H. Chen and D. L. Jiang, *Science*, 2017, **357**, 673-676; Y. H. Jin, Y. M. Hu and W. Zhang, *Nat. Rev. Chem.*, 2017, **1**; L. L. Li, S. Liu, Q. Zhang, N. T. Hu, L. M. Wei, Z. Yang and H. Wei, *Acta Physico-Chimica Sinica*, 2017, **33**, 1960-1977; R. F. Chen, J. L. Shi, Y. Ma, G. Q. Lin, X. J. Lang and C. Wang, *Angew. Chem. Int. Ed.*, 2019, **58**, 6430-6434.

7 N. Huang, P. Wang and D. L. Jiang, *Nat. Rev. Mater.*, 2016, **1**.

8 A. P. Côté, A. I. Benin, N. W. Ockwig, M. O'Keeffe, A. J. Matzger and O. M. Yaghi, *Science*, 2005, **310**, 1166-1170.

9 Y. Du, H. S. Yang, J. M. Whiteley, S. Wan, Y. H. Jin, S. H. Lee and W. Zhang, *Angew. Chem. Int. Ed.*, 2016, **55**, 1737-1741; J. Q. Lv, Y. X. Tan, J. F. Xie, R. Yang, M. X. Yu, S. S. Sun, M. D. Li, D. Q. Yuan and Y. B. Wang, *Angew. Chem. Int. Ed.*, 2018, **57**, 12716-12720.

10 S. L. Lu, Y. M. Hu, S. Wan, R. McCaffrey, Y. H. Jin, H. W. Gu and W. Zhang, *J. Am. Chem. Soc.*, 2017, **139**, 17082-17088.

11 Z. P. Li, Y. F. Zhi, P. P. Shao, H. Xia, G. S. Li, X. Feng, X. Chen, Z. Shi and X. M. Liu, *Applied Catalysis B-Environmental*, 2019, **245**, 334-342; Y. C. Wang, H. Liu, Q. Y. Pan, C. Y. Wu, W. B. Hao, J. Xu, R. Z. Chen, J. Liu, Z. B. Li and Y. J. Zhao, *J. Am. Chem. Soc.*, 2020, **142**, 5958-5963; X. Han, Q. C. Xia, J. J. Huang, Y. Liu, C. X. Tan and Y. Cui, *J. Am. Chem. Soc.*, 2017, **139**, 8693-8697; G. Q. Lin, H. M. Ding, R. F. Chen, Z. K. Peng, B. S. Wang and C. Wang, *J. Am. Chem. Soc.*, 2017, **139**, 8705-8709.

12 J. W. Colson, A. R. Woll, A. Mukherjee, M. P. Levendorf, E. L. Spitler, V. B. Shields, M. G. Spencer, J. Park and W. R. Dichtel, *Science*, 2011, **332**, 228-231; H. M. Ding, J. Li, G. H. Xie, G. Q. Lin, R. F. Chen, Z. K. Peng, C. L. Yang, B. S. Wang, J. L. Sun and C. Wang, *Nature Communications*, 2018, **9**, 5234.

13 O. M. Yaghi, M. O'Keeffe, N. W. Ockwig, H. K. Chae, M. Eddaoudi and J. Kim, *Nature*, 2003, **423**, 705-714; S. Kitagawa, R. Kitaura and S. Noro, *Angew Chem Int Ed Engl*, 2004, **43**, 2334-2375; Q. Wang and D. Astruc, *Chem. Rev.*, 2020, **120**, 1438-1511.

14 H. Furukawa, K. E. Cordova, M. O'Keeffe and O. M. Yaghi, *Science*, 2013, **341**, 974.

15 O. M. Yaghi and H. L. Li, *J. Am.Chem. Soc*, 1995, **117**, 10401−10402.

16 H. Furukawa and O. M. Yaghi, *J. Am. Chem. Soc.*, 2009, **131**, 8875-8883; H. C. Zhou, J. R. Long and O. M. Yaghi, *Chem. Rev.*, 2012, **112**, 673-674; H. C. Zhou and S. Kitagawa, *Chem Soc Rev*, 2014, **43**, 5415-5418; C. R. Kim, T. Uemura and S. Kitagawa, *Chem. Soc. Rev.*, 2016, **45**, 3828-3845; X. Y. Feng, Y. H. Pi, Y. Song, C. Brzezinski, Z. W. Xu, Z. Li and W. B. Lin, *J. Am. Chem. Soc.*, 2020, **142**, 690-695.

17 C. J. Zhang and F. F. Li, *J. Phys. Chem. A*, 2012, **116**, 9123-9130; C. J. Zhang, D. X. Ma, S. N. Yang and J. X. Liang, *ACS Omega*, 2016, **1**, 620-625.

18 X. F. Jia and C. J. Zhang, *Comput. Theor. Chem.*, 2016, **1075**, 47-53; D. X. Ma and C. J. Zhang, *Comput. Theor. Chem.*, 2017, **1115**, 30-36; D. X. Ma, C. J. Zhang, Z. N. Chen and X. Xu, *Phys. Chem. Chem. Phys.*, 2017, **19**, 2417-2424.

19 C. J. Zhang, F. Fan, Z. M. Wang, J. S. Song, C. S. Li and Y. Mo, *Chem. Eur. J.*, 2018, **24**, 10216-10223; C. J. Zhang, Z. M. Wang, J. S. Song, C. S. Li and Y. R. Mo, *Theor. Chem. Acc.*, 2019, **138**.

20 K. Thirumoorthy, A.Karton, V. S. Thimmakondu, *J. Phys. Chem. A*, 2018, **122**, 9054–9064.

21 D. Andrae, U. U. Häußermann, M. Dolg, H. Stoll and H. Preuß, *Theor. Chim. Acta* 1990, **77**, 123-141.

22 A. D. McLean, G. S. Chandler, *J. Chem. Phys.*, **1980**, 72, 5639−5648; R. Krishnan, J. S. Binkley, R. Seeger, J. A. Pople, *J. Chem. Phys.*, **1980**, 72, 650−654; L. A. Curtiss, M. P. McGrath, J. P. Blaudeau, N. E. Davis, R. C. Binning, L. Radom, *J. Chem. Phys.*, **1995**, 103, 6104−6113.

23 A. D. Becke, *J. Chem. Phys.*, **1993**, 98, 5648-5652.

24 Y, Zhao, D. G. Truhlar, Theor. Chem. Acc., **2008**, 120, 215−241.

25 R. Krishnan, J. S. Binkley, R. Seeger, J. A. Pople, *J. Chem. Phys.*, **1980**, 72, 650−654; A. D. McLean, G. S. Chandler, *J. Chem. Phys.*, **1980**, 72, 5639−5648; L. A. Curtiss, M. P. McGrath, J. P. Blaudeau, N. E. Davis, R. C. Binning, L. Radom, *J. Chem. Phys.*, **1995**, 103, 6104−6113.

26 E. D. Glendening, J. K. Badenhoop, A. E. Reed, J. E. Carpenter, J. A. Bohmann, C. M. Morales and F. Weinhold, *NBO Version 5.0*, (2001) Theoretical Chemistry Institute, University of Wisconsin, Madison, WI.

27 M. J. Frisch, G. W. Trucks, H. B. Schlegel, G. E. Scuseria, M. A. Robb, J. R. Cheeseman, G. Scalmani, V. Barone, B. Mennucci, G. A. Petersson, H. Nakatsuji, M. Caricato, X. Li, H. P. Hratchian, A. F. Izmaylov, J. Bloino, G. Zheng, J. L. Sonnenberg, M. Hada, M. Ehara, K. Toyota, R. Fukuda, J. Hasegawa, M. Ishida, T. Nakajima, Y. Honda, O. Kitao, H. Nakai, T. Vreven, J. Montgomery, J. A. , J. E. Peralta, F. Ogliaro, M. Bearpark, J. J. Heyd, E. Brothers, K. N. Kudin, V. N. Staroverov, T. Keith, R. Kobayashi, J. Normand, K. Raghavachari, A. Rendell, J. C. Burant, S. S. Iyengar, J. Tomasi, M. Cossi, N. Rega, J. M. Millam, M. Klene, J. E. Knox, J. B. Cross, V. Bakken, C. Adamo, J. Jaramillo, R. Gomperts, R. E. Stratmann, O. Yazyev, A. J. Austin, R. Cammi, C. Pomelli, J. W. Ochterski, R. L. Martin, K. Morokuma, V. G. Zakrzewski, G. A. Voth, P. Salvador, J. J. Dannenberg, S. Dapprich, A. D. Daniels, O. Farkas, J. B. Foresman, J. V. Ortiz, J. Cioslowski and D. J. Fox, *Gaussian 09*, (2010) Gaussian, Inc., Wallingford CT.

28 R. Hoffmann, R. W. Alder and C. F. Wilcox, *J. Am. Chem. Soc.*, 1970, **92**, 4992-4993.

29 R. Keese, *Chem. Rev.*, 2006, **106**, 4787-4808; G. Merino, M. A. Mendez-Rojas, H. I. Beltraan, C. Corminboeuf, T. Heine, A. Vela, *J. Am. Chem. Soc.*, **2004**, 126, 16160-16169; Y. Sahin, M. Hartmann, G. Geiseler, D. Schweikart, C. Balzereit, G. Frenking, W. Massa, A. Berndt, *Angew. Chem. Int. Edit.*, **2001**, 40, 2662-2665; L. S. Wang, A. I. Boldyrev, X. Li, J. Simons, J. Am. Chem. Soc., **2000**, 122, 7681-7687; J. Xu, X. X. Zhang, S. Yu, Y. H. Ding, K. H. Bowen, *J Phys Chem Lett.*, **2017**, 8, 2263-2267; C. J. Zhang, W. X. Sun, Z. X. Cao, *J. Am. Chem. Soc.*, **2008**, 130, 5638-5639.